Physics Letters A 375 (2011) 628–632

Contents lists available at ScienceDirect

Physics Letters A

www.elsevier.com/locate/pla

Vortex polarity in 2-D magnetic dots by Langevin dynamics simulations

Ph. Depondt [a,*], J.-C.S. Lévy [b], F.G. Mertens [c]

[a] Institut des NanoSciences de Paris, Université Pierre et Marie Curie, UMR 7588 CNRS, 75252 Paris Cedex 05, France
[b] Matériaux et Phénomènes Quantiques, Université Denis Diderot, UMR 7162 CNRS, 75013 Paris, France
[c] Physikalisches Institut, Universität Bayreuth, D-95440 Bayreuth, Germany

ARTICLE INFO

Article history:
Received 16 April 2010
Received in revised form 3 November 2010
Accepted 16 December 2010
Available online 21 December 2010
Communicated by R. Wu

Keywords:
Magnetic properties and materials
Numerical simulation studies
Magnetic properties of nanostructures

ABSTRACT

Two-dimensional magnetic plots of finite size were simulated by integrating the Landau–Lifshitz equation for the isotropic Heisenberg model with a systematic exploration of the effect of dipole–dipole interactions of various strengths d, at a low temperature. Structures with or without vortices are observed, and in the cases in which vortices are present, out-of-plane contributions show only for relatively weak dipolar strengths: the integrated intensity of the out-of-plane component decreases roughly as $1/d$ with increasing dipolar strength while the vortex core width decreases as $d^{-\frac{1}{2}}$. The coexistence of several vortices with an out-of-plane component seems limited to a narrow d-range, at least for the sample sizes studied. The size limit below which the vortices disappear decreases roughly as $1/d$.

1. Introduction and model

Vortices and other topological defects have been suggested by theory [1], Monte Carlo [2–5] simulations, micromagnetic simulations [6] and also experimentally observed in magnetic two-dimensional dots [7–9]. Analytical work based on Taylor expansions [10] again shows that dipolar interactions generate magnetic topological defects. The issue of data storage is clearly essential in such interest and, specifically, the polarity of vortices *i.e.* the out-of-plane spin component associated with a vortex (*e.g.* [11]) can be manipulated. This, however, assumes the presence of such polarity. We present Langevin spin dynamics simulations [12] with dipolar interaction competing with nearest neighbour exchange which enable to study both spin structures, and, when present, vortex polarity, for various dipolar strengths and several dot sizes.

We solve the usual Landau–Lifshitz spin-dynamics equation:

$$\dot{\mathbf{s}}_\ell = -\mathbf{s}_\ell \times \mathbf{H}_\ell, \quad \mathbf{H}_\ell = \mathbf{H}_{H_\ell} + \mathbf{H}_{d_\ell} \tag{1}$$

where $\mathbf{s}_\ell$ is the vector associated with spin ℓ and $\mathbf{H}_\ell$ the local field which is caused by all the other spins. The local field is the sum of two terms, where the first is a nearest-neighbour Heisenberg or exchange interaction, the second the dipole–dipole interaction; thus:

$$\mathbf{H}_{H_\ell} = \mathbf{J} \sum_{\substack{\ell' \\ (\text{neighbour } \ell)}} \mathbf{s}_{\ell'}$$

$$\mathbf{H}_{d_\ell} = d \sum_{\substack{\ell' \\ (\ell' \neq \ell)}} \left(3 \frac{\mathbf{s}_{\ell'} \cdot \mathbf{r}_{\ell\ell'}}{|\mathbf{r}_{\ell\ell'}|^2} \mathbf{r}_{\ell\ell'} - \mathbf{s}_{\ell'} \right) \frac{1}{|\mathbf{r}_{\ell\ell'}|^3}$$

$\mathbf{J}$ being, in this case, the identity matrix for the isotropic Heisenberg model. The strength of the dipole–dipole interaction is d and $\mathbf{r}_{\ell\ell'}$ is the vector connecting spins ℓ and ℓ'.

The simulated samples are square monolayers of identical spins on a rigid square lattice, (32×32), (64×64) or (128×128), in the xOy plane. The spins are free to rotate with $|\mathbf{s}_\ell(t)| = 1$, $\forall \ell$, $\forall t$. The integration procedure is the same as in Ref. [12]: for every timestep, each spin explicitly precesses around the local field via a rotation matrix which conserves $|\mathbf{s}_\ell(t)|$, and a Langevin dynamics allows to introduce temperature. The dipole–dipole interaction is dealt with using the convolution theorem and Fast Fourier Transforms: this introduces no additional approximation through zero-padding and the discrete character of the sample (see [12] and references therein).

These methods were checked in [12] for a X–Y Heisenberg model ($J_x = J_y = 1$, $J_z = 0$) without dipolar interaction ($d = 0$) and with $d = 0.2$ with varying temperatures: a variety of in-plane structures with or without vortices and vortex–antivortex pairs were observed, along with the associated dynamics.

We deal here with the isotropic Heisenberg model ($J_x = J_y = J_z = 1$), low temperature $T = 0.001$ in reduced units (in these units, the Kosterlitz–Thouless transition for the X–Y Heisenberg model [13,14] takes place for $T \simeq 0.7$), and varying dipole–dipole

* Corresponding author.
E-mail addresses: depondt@insp.jussieu.fr (Ph. Depondt), jean-claude.levy@univ-paris-diderot.fr (J.-C.S. Lévy), franz.mertens@uni-bayreuth.de (F.G. Mertens).

0375-9601/$ – see front matter
doi:10.1016/j.physleta.2010.12.041

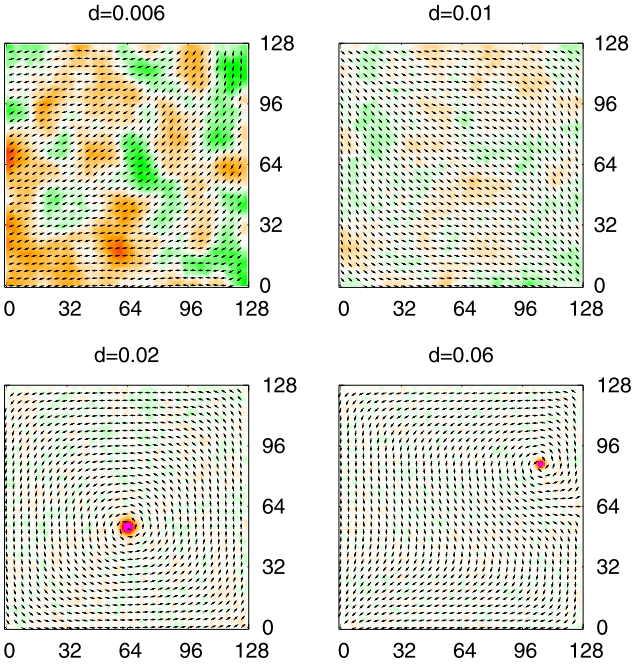

Fig. 1. Instantaneous 128×128 configurations, $d = 0.006$, 0.01, 0.02, and 0.06, $T = 0.001$. Arrows represent the in-plane orientations of spins (a sampling of one out of four spins in both directions to avoid overcrowding of the figure). The color scheme indicates the out-of-plane component; the colors follow the sequence: blue, cyan, green, white, orange, red, magenta for s_z ranging from -0.5 to $+0.5$, thus the first three colors correspond to negative polarization, white to no polarization and the last three to positive polarization. (For interpretation of the references to colour in this figure legend, the reader is referred to the web version of this Letter.)

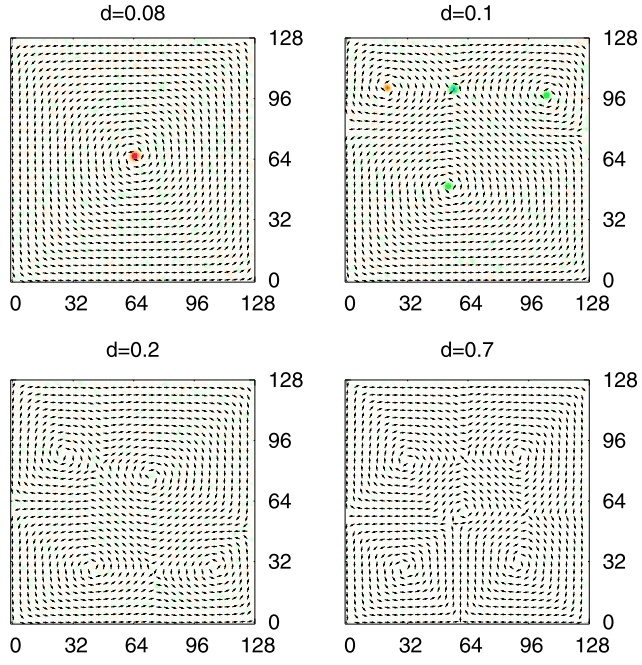

Fig. 2. Instantaneous configurations for $d = 0.08$, 0.1, 0.2 and 0.7, $T = 0.001$. Arrows and colors have the same meaning as in Fig. 1.

strength: $0.001 \leqslant d \leqslant 0.9$, a way to change the ratio d/J or exchange length $\sqrt{J/d}$. The choice of a low but finite temperature is a compromise: we want to limit thermal fluctuations so that significant features are not blurred beyond detection, but on the other hand, we wish to let the system explore available phase space in order to avoid getting trapped in some metastable state. These requirements are far from trivial as will be seen in Section 2.

All simulations, unless otherwise specified, were done in the following manner: an initial, highly disordered configuration was chosen and a first relaxation run with strong damping was carried out; a second relaxation run was then performed with small (0.0005) damping and a final production run was done with the same small damping.

2. Configurations

2.1. Instantaneous configurations

Typical configurations are shown on Figs. 1 and 2 for (128×128) samples only, since (32×32) and (64×64) yield quite similar configurations as the polarity effect is restricted to a small number of sites in the close vicinity of the vortex core.

For small dipolar interaction $d < 0.01$ (see $d = 0.006$ and 0.01 in Fig. 1, top), vortices are not observed but the in-plane configuration is non-uniform. A relatively strong ($|s_z| \approx 0.1$) "wavy", out-of-plane spin component is present; if, instead of showing snapshots as in Fig. 1, one averages over time, these waves disappear, meaning they are thermal fluctuations, namely, for small dipolar interaction, the low-frequency gap in the magnon dispersion curve (see [12]) vanishes and long wavelength, low frequency modes can occur even at very low temperatures. It was shown in [10], using a Taylor series expansion, that dipole–dipole interactions lead to anisotropy: the overall out-of-plane contribution therefore decreases as d increases because of the increasing demagnetizing field. In-plane configurations define, at the edges a sort of "leaf" configuration [6]: spins located next to the edges of the sample tend to lie parallel to these edges because of the dipolar interaction, while bulk spins tend to lie in a direction parallel to the diagonal of the square, thus giving an overall impression of a, maybe poplar, leaf (see Fig. 1, top right).

For intermediate dipolar interaction, *i.e.* $0.01 < d \leqslant 0.08$ as observed from Figs. 1 ($d = 0.02$ and 0.06) and 2 ($d = 0.08$), usually one vortex appears with a significant out-of-plane spin contribution at the vortex core, while $|s_z|$ remains negligible elsewhere.

For large enough dipolar interaction *i.e.* $0.08 < d < 0.2$ (Fig. 2), several vortices appear. The individual vortex width decreases but the vortex heights also decrease. The out-of-plane components finally disappear completely for $d \sim 0.1$.

For very large dipolar interaction $d \geqslant 0.2$, configurations remain in-plane as in the XY case [12] and vortices constitute a relatively ordered structure. Boundaries in which the spin orientations change abruptly connect vortices in a way reminiscent of Monte Carlo simulations [18]. However, the Monte Carlo simulations were done on a hexagonal lattice resulting in patterns with that symmetry, while ours, on a square lattice, tend to retain right angles, thus showing the importance of doing microscopic simulations in which the lattice is explicit.

2.2. Are these ground states?

For large d (approx. for $d \geqslant 0.08$), convergence is rapid and no inconsistency was detected. However, the snapshot shown for $d = 0.06$ (Fig. 1, bottom right), at least, is clearly not a ground state: the vortex is not in the middle of the sample where symmetry would require it to be. It is known [15] that a non-central vortex migrates toward the center via a gyrotropic motion: for small dipolar interaction, this motion is very slow, and, in this instance, not completed. Thus the question of whether our configurations can be considered to represent ground states should be addressed: several tests were therefore done with different initial conditions, namely (1) a uniform configuration in which all spins are parallel in-plane and (2) with a single central vortex. These configurations were left to relax in the usual manner, in order to let, for instance,

Table 1
Time-averaged energies per site after relaxation for simulations started with initial conditions: (1) uniform in-plane spin orientations and (2) single central vortex. δ is the difference between the energy of the central vortex structure and the energy of the uniform structure. When $\delta > 0$, the uniform state is more stable, and when $\delta < 0$ the single central vortex state is more stable. The system does not spontaneously switch from one structure to the other. The value of the dipolar strength d_c for which δ changes sign can be obtained via interpolation with $d_c = 0.105$ (32×32), 0.058 (64×64), 0.032 (128×128) and 0.016 (256×256), which can be fitted with a power law: $d_c = 2.09\ell^{-0.86}$ where $\ell = 32$, 64, 128 or 256.

Size	32×32		
d	Uniform	Central vortex	δ
0.01	−3.9129	−3.8956	0.01735
0.02	−3.9537	−3.9372	0.01649
0.03	−3.9948	−3.9797	0.01508
0.04	−4.0362	−4.0227	0.01341
0.05	−4.0775	−4.0659	0.01161
0.06	−4.1180	−4.1093	0.00866
0.07	−4.1598	−4.1529	0.00686
0.08	−4.2016	−4.1966	0.00499
0.09	−4.2435	−4.2404	0.00307
0.1	−4.2855	−4.2843	0.00114
0.11	−4.3274	−4.3283	−0.00084
0.12	−4.3694	−4.3723	−0.00294

Size	64×64		
d	Uniform	Central vortex	δ
0.01	−3.9779	−3.9734	0.00455
0.02	−4.0210	−4.0173	0.00376
0.03	−4.0643	−4.0614	0.00291
0.04	−4.1077	−4.1058	0.00191
0.05	−4.1510	−4.1502	0.00086
0.06	−4.1945	−4.1947	−0.00021
0.07	−4.2379	−4.2392	−0.00127
0.08	−4.2814	−4.2838	−0.00236

Size	128×128		
d	Uniform	Central vortex	δ
0.01	−4.0107	−4.0096	0.00113
0.02	−4.0549	−4.0543	0.00061
0.03	−4.0992	−4.0991	0.00011
0.04	−4.1435	−4.1439	−0.00041
0.05	−4.1878	−4.1888	−0.00102

Size	256×256		
d	Uniform	Central vortex	δ
0.01	−4.02698	−4.02684	0.00014
0.02	−4.07175	−4.07184	−0.00009

an out-of-plane component emerge. Despite attempts with varying relaxation times and dampings, it turns out that in none of these simulations would the system spontaneously switch from one structure to another: the uniform samples all remained devoid of vortices after relaxation, while the single vortex samples all ended up as single vortex final states, even for small 32×32 samples. It can, of course, be argued that the durations accessible to our simulations are too short; however, the system energies can be monitored (after relaxation) in both situations, compared in order to decide which structure has lowest energy and declare it is likely to be the ground state. The result of this procedure is given on Table 1 where quantity δ is the difference between the energy of the central vortex state and the energy of the uniform state.

For 128×128 samples, the value of d for which the most stable structure changes from uniform to single vortex is 0.032: this means that on Fig. 1, the snapshot for $d = 0.02$ does not show a ground state as the uniform configuration has lower energy, while for $d = 0.06$, the vortex will simply proceed slowly towards the center to a ground state. It should be noted that the energy differences between the two structures remain small although above thermal fluctuations at this temperature.

2.3. Vortex polarity

The out-of-plane vortex-core contributions thus appear in the intermediate d range and were fitted when present (Fig. 3) with a Gaussian function: the height remains constant and slightly less than 1 for $d < 0.08$ while the width decreases roughly as $1/\sqrt{d}$, meaning that the integrated intensity of the out-of-plane vortex components decreases roughly as $1/d$.

2.4. The effect of size

No major difference between the three samples of different sizes is to be observed. However the appearance of a vortex for increasing d occurs for smaller d in the larger samples (I to II in Fig. 4): the critical size roughly varies as $d^{-\frac{1}{0.86}}$ following the results of Table 1. The d-range for which several vortices are present in the sample with non-zero polarity is narrow (Figs. 1 and 2): for these sample sizes, data storage via multi-vortex polarity might turn out to be uneasy, larger samples would be necessary.

3. Analysis and conclusion

We thus summarize our results in the following way. The equilibrium configurations are, as usual, obtained through the competition between the exchange (or Heisenberg) field $\mathbf{H}_{H,\ell}$ and the dipolar field $\mathbf{H}_{d,\ell}$ in Eq. (1): the exchange field tends to have all spins parallel while the dipolar field favors loops which can only reside in-plane in a 2-D system. When there is no dipolar field, the exchange term of course wins: spins are all parallel, but in any direction (in-plane, out-of-plane, or whatever) in the isotropic case. When the dipolar field is strong enough to overcome exchange, we obtain in-plane vortices [16].

For very small values of d ($d \approx 0.002$), the spins escape in the third dimension, nearly freely. When d is increased, this escape is restricted to the vicinity of the vortex core and is more and more reduced. Indeed, the interesting case resides in the intermediate range when one or several vortices appear: whenever a vortex is present, the exchange part will tend to reduce the nearest neighbour spin–spin angles, so it makes the spins stick out-of-plane. This of course costs energy because we cannot have out-of-plane loops (in 2-D) to satisfy the dipolar term (this is why the dipolar term produces an effective anisotropy [17], as it will tend to pull all spins back in-plane). We can try roughly to evaluate the relevant quantities that monitor this competition in a single-vortex configuration.

The out-of-plane exchange field component will be, for a spin within the area with an out-of-plane component surrounding a vortex, the sum of the z-components of its four neighbour spins,

$$H_{Hz,\ell} = J_z \sum_{\substack{\ell' \\ (\text{neighbour } \ell)}} s_{z,\ell'}$$

Since nearest neighbours will have reasonably similar orientations, this is roughly proportional to $s_{z,\ell}$, its own out-of-plane component:

$$H_{Hz,\ell} \simeq J_z C_H s_{z,\ell}$$

where C_H is a constant.

Now, the out-of-plane component of the dipolar field is *not* reduced to nearest neighbours, but is a sum of all the contributions of the spins surrounding a vortex, within the area where they have out-of-plane components:

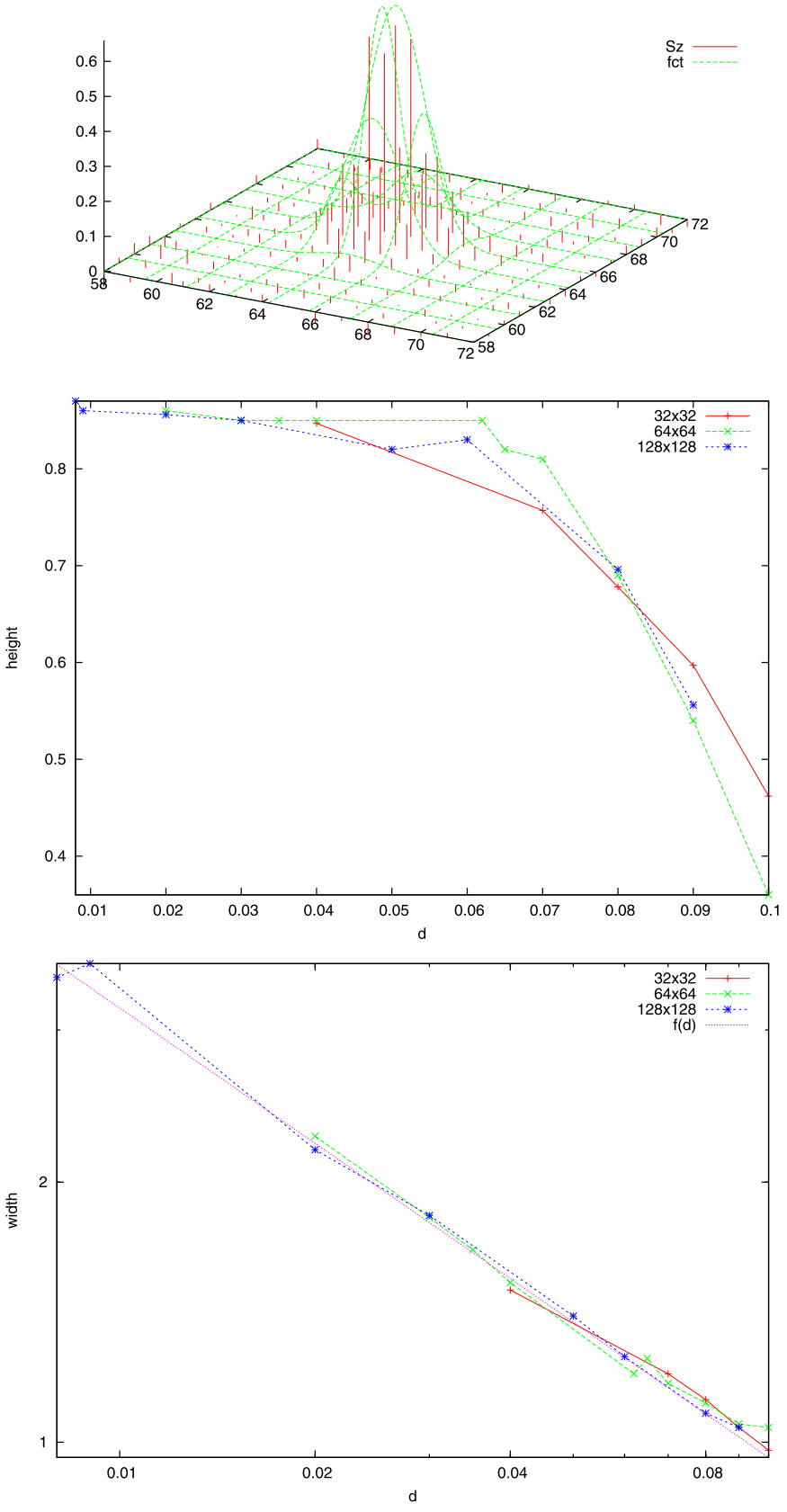

Fig. 3. Results of fitting a Gaussian function to the out-of-plane contribution to magnetization at vortex cores for system sizes (32×32), (64×64) and (128×128). Top: fit example for $d = 0.08$ (red: s_z, green: Gaussian); middle: height of the Gaussian; bottom: width of the Gaussian and function $f(d) = ad^{-b}$, $a = 0.29 \pm 0.03$, $b = 0.52 \pm 0.022$ (logarithmic scales). (For interpretation of the references to colour in this figure legend, the reader is referred to the web version of this Letter.)

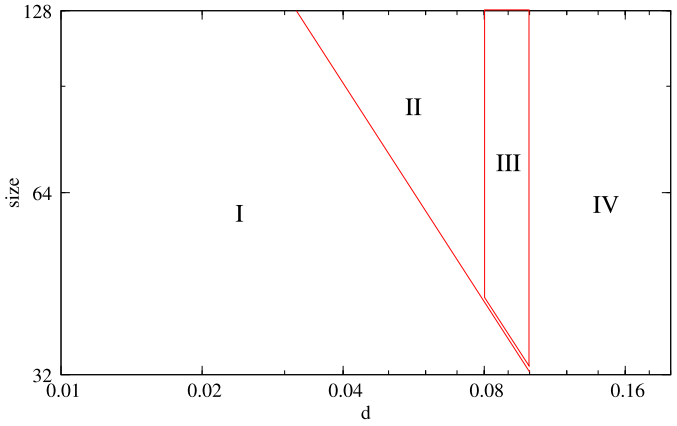

Fig. 4. Summary of structures obtained for varying system size and dipolar strength (log–log plot): phase I stands for the no-vortex phase, II for the single vortex, with polarity (or with out-of-plane component) phase, III for multi-vortex, polarity phase and IV for multi-vortex in-plane. The line between I and II roughly represents a $d^{-\frac{1}{0.86}}$ dependence from Table 1.

$$H_{dz,\ell} \simeq dC_d \sum_{\substack{\ell' \\ (\text{vortex}\,\ell)}} s_{z,\ell'}$$

where C_d is a geometrical constant and the sum extends over all spins within the same vortex surrounding. This is d times the integrated intensity of the out-of-plane contributions within the vortex, or, again roughly

$$H_{dz,\ell} \simeq dC_d P_{z,\ell}$$

where $P_{z,\ell}$ is the integrated out-of-plane intensity of the vortex that contains spin ℓ,

$$P_{z,\ell} \propto 2\pi s_{z,\ell} \int_0^\infty \mathrm{e}^{-\frac{r^2}{2\rho^2}} r\,dr = 2\pi s_{z,\ell}\rho^2$$

where ρ is the width of the Gaussian function of Fig. 3. Equilibrium is reached when both terms, exchange and dipolar, are equal,

$$J_z s_{z,\ell} = d s_{z,\ell}\,\rho^2 C$$

where C is a roughly constant coefficient which includes all the previous ones; $s_{z,\ell}$ drops out, and

$$\rho^2 \propto 1/d$$

as obtained in Fig. 3. This result is essentially the consequence of the non-locality of the dipolar interaction as opposed to the locality of the exchange term: dipoles, so-to-say, join forces beyond nearest neighbours in order to force a vortex to appear; when ρ drops below the lattice constant, it means that the dipoles are locally strong enough to overcome the exchange interactions. This is the case for large dipolar interaction configurations with several vortices for which the exchange term cannot impose significant out-of-plane components.

The out-of-plane component of vortices only occurs in an intermediate range of dipolar interactions. The lower boundary is given by the limit when vortices can appear: this limit decreases to smaller values of d with the size of the simulated sample as the effects of dipolar interactions add up on the whole sample, while the exchange term is local. The upper boundary occurs when the dipole–dipole interaction is locally strong enough to force spins in-plane: this limit does not appear to depend on size, as it is local. The d-range of co-existence of out-of-plane polarity and a multivortex configuration seems to be rather narrow for the sample sizes studied here.

The issue of whether we are dealing here with ground states, as we should if we are claiming to provide a phase diagram, was addressed. Several symptoms are to be pointed out: firstly the configuration for $d = 0.06$ in Fig. 1 cannot be a ground state because of symmetry since the vortex is not central and, secondly, the energy (Table 1) shows little sensitivity to configuration changes. This infers that many "ground states" with the same energy, or almost the same energy, exist, as in spin glasses in which a large number of nearly degenerate states are separated by energy barriers. Such frustration is general in dipolar systems, even without random interactions, be it magnetic systems (*e.g.* [19]), or liquid crystals (*e.g.* [20]). This creates a technical problem as we can never be quite sure we are studying the ground state: the obvious compromise is to work at finite temperature in order to allow the system to explore, at least partially, the available phase space, but low enough to avoid too large fluctuations that would blur significant features. The relaxation procedure from a highly disordered initial state mentioned at the end of Section 1, is a form of annealing which also is classic in dealing with frustration, however it requires cautious handling.

References

[1] P.I. Belobrov, V.A. Voevodin, V.A. Ignatchenko, Sov. Phys. JETP 61 (1985) 522.
[2] E.Y. Vedmedenko, A. Ghazali, J.-C.S. Lévy, Surf. Sci. 402 (1998) 391.
[3] E.Y. Vedmedenko, H.P. Oepen, A. Ghazali, J.-C.S. Lévy, J. Kirschner, Phys. Rev. Lett. 84 (2000) 5884.
[4] J. Sasaki, F. Matsubara, J. Phys. Soc. Japan 66 (1997) 2138.
[5] J.C. Rocha, P.Z. Coura, S.A. Leonel, R.A. Rias, B.V. Costa, J. Appl. Phys. 107 (2010) 053903.
[6] R.P. Cowburn, M.E. Welland, Phys. Rev. B 58 (1998) 9217.
[7] A. Vaterlaus, C. Stamm, U. Maier, M.G. Pini, P. Politi, D. Pescia, Phys. Rev. Lett. 84 (2000) 2247.
[8] J. Li, C. Rau, Phys. Rev. Lett. 97 (2006) 107201.
[9] J.E. Villegas, C.P. Li, I.K. Schuller, Phys. Rev. Lett. 99 (2007) 227001.
[10] J.-C.S. Lévy, Phys. Rev. B 63 (2001) 104409.
[11] M. Tanase, A.K. Petford-Long, O. Heinonen, K.S. Buchanan, J. Sort, J. Nogués, Phys. Rev. B 79 (2009) 014436.
[12] P. Depondt, F.G. Mertens, J. Phys.: Condens. Matter 21 (2009) 336005.
[13] J.M. Kosterlitz, J.D. Thouless, J. Phys. C: Solid St. Phys. 6 (1973) 1181.
[14] J.M. Kosterlitz, J. Phys. C: Solid St. Phys. 7 (1974) 1046.
[15] K.Yu. Guslienko, B.A. Ivanov, V. Novosad, Y. Otani, H. Shima, K. Fukamichi, J. Appl. Phys. 91 (2002) 8037.
[16] D.D. Stancil, Theory of Magnetostatic Waves, Springer Verlag, 1993.
[17] J.G. Caputo, Y. Gaididei, V. Kravchuk, F.G. Mertens, D. Sheka, Phys. Rev. B 76 (2007) 174428.
[18] E.Y. Vedmedenko, A. Ghazali, J.-C.S. Lévy, Phys. Rev. B 59 (1999) 3329.
[19] W. Kleeman, O. Petracic, Ch. Binek, G.N. Kakazei, Y.G. Pogorelov, J.B. Sousa, S. Cardoso, P.P. Freitas, Phys. Rev. B 63 (2001) 134423.
[20] W. Józefowicz, L. Longa, Phys. Rev. E 76 (2007) 011701.